Full-potential linearized augmented-plane-wave calculation of the magneto-optical Kerr effect in Fe, Co and Ni

1999 J. Phys.: Condens. Matter 11 6301

(http://iopscience.iop.org/0953-8984/11/32/320)

J. Phys.: Condens. Matter **11** (1999) 6301–6309. Printed in the UK PII: S0953-8984(99)03054-4

Full-potential linearized augmented-plane-wave calculation of the magneto-optical Kerr effect in Fe, Co and Ni

J Kuneš and P Novák

Institute of Physics, Academy of Sciences, Cukrovarnická 10, 162 53 Praha 6, Czech Republic

Received 24 March 1999, in final form 8 June 1999

Abstract. The magneto-optical Kerr effect (MOKE) is calculated for bcc Fe, hcp Co and fcc Ni using the full-potential linearized augmented-plane-wave method. The results are compared with the available experimental and computational data obtained previously in other studies and rather close agreement is achieved with earlier, non-full-potential calculations of Oppeneer *et al* (Oppeneer P M, Maurer T, Sticht J and Kübler J 1992 *Phys. Rev.* B **45** 10 924, Oppeneer P M, Sticht J, Maurer T and Kübler J 1992 *Z. Phys.* B **88** 309). Careful analysis of the influence of the input parameters on the theoretical MOKE spectra is performed. Results obtained with two different forms of the exchange–correlation potential (local density and generalized gradient approximation) and with a Hamiltonian including the orbital polarization term are presented.

1. Introduction

During recent decades the magneto-optical Kerr effect (MOKE) has attracted the attention of physicists in view of its application in data storage technology as well as its being a sensitive tool for exploration of electronic structure. The first step towards *ab initio* calculation of the MOKE was made by Wang and Callaway [1], who calculated the absorptive part of the off-diagonal matrix element of the conductivity tensor for Ni. But only recently have several papers appeared in which realistic calculations of the MOKE based on the density functional theory were presented [2,4,11,13,18,19]. Although the calculation of MOKE spectra from the known band structure is quite straightforward, different methods of band-structure calculation may yield contradictory results. In particular the MOKE for Fe, Co and Ni calculated by the full-potential method [4] differs substantially from the results obtained with the potential which is spherically averaged [2]. The MOKE is sensitive to the details of the electronic structure, which in turn depends on the parameters of the calculation—the number of k-points, energy cut-offs etc. It is therefore desirable to analyse carefully the dependence of the calculated spectra on these parameters in order to ascertain that the results are stable within a given method. To our knowledge such detailed analysis was performed only for the augmented-spherical-wave (ASW) calculation [2], in which the spherically averaged potential is used.

In this paper we present a calculation of the MOKE based on the full-potential linearized augmented-plane-wave (FPLAPW) method as implemented in the WIEN97 code [5]. WIEN97 is a well tested and commonly used code for calculation of the electronic structure. In order to calculate the MOKE spectra we have modified the package OPTIC so that calculation of the off-diagonal elements of the conductivity tensor for a system with spin–orbit coupling was possible. We have also written a new package LAPWORB which enables self-consistent inclusion of the orbital polarization into the Hamiltonian and which we briefly describe in this

0953-8984/99/326301+09$30.00

paper. The resulting program is applied to calculate the MOKE for fcc Ni, hcp Co and bcc Fe. The results are compared with those obtained by the ASW method [2, 19] and with the experimental data. The dependence of the MOKE on the parameters of the FPLAPW method is carefully analysed. We also study the effect of the choice of the exchange–correlation potential and the inclusion of the orbital polarization term into the Hamiltonian.

2. Theory

The magneto-optical Kerr effect is described by a complex parameter Φ_K which carries the information about the Kerr rotation and ellipticity. This parameter depends on the experimental arrangement. The results we present correspond to the polar Kerr effect, i.e. a configuration in which the incident beam is collinear with the sample magnetization and both are perpendicular to the sample surface. In this arrangement the Kerr rotation Θ_K and the ellipticity ε_K are given by

$$\Phi_K(\omega) = \Theta_K(\omega) + \mathrm{i}\varepsilon_K(\omega) = -\frac{\sigma_{xy}(\omega)}{\sigma_{xx}(\omega)}\left(1 + \frac{4\pi\,\mathrm{i}}{\omega}\sigma_{xx}(\omega)\right)^{-1/2} \tag{1}$$

where $\sigma_{\alpha\beta}$ are the matrix elements of the conductivity tensor. The conductivity tensor can be expressed as a sum of two contributions, called interband and intraband. We do not consider the intraband contribution in the results presented for two reasons. First, the influence of the intraband effects is usually described by the phenomenological Drude model. As we primarily want to compare our results to other *ab initio* computations it is appropriate to compare interband contributions only. Second, the intraband contribution affects the MOKE spectra of 3d metals only at low energies (under 1 eV) and does not change the shapes of the curves, so comparison to the experiment remains possible. For evaluation of the interband conductivity, the following expression [1, 3] was used:

$$\sigma_{\alpha\beta}(\omega) = \frac{\mathrm{i}e^2}{m^2\hbar\Omega}\sum_{\boldsymbol{k}}\sum_{\substack{m\ \mathrm{occ}\\ n\ \mathrm{un}}}\frac{1}{\omega_{nm}(\boldsymbol{k})}\left(\frac{\Pi^{\alpha}_{mn}\Pi^{\beta}_{nm}}{\omega - \omega_{nm}(\boldsymbol{k}) + \mathrm{i}\delta} + \frac{(\Pi^{\alpha}_{mn}\Pi^{\beta}_{nm})^*}{\omega + \omega_{nm}(\boldsymbol{k}) + \mathrm{i}\delta}\right). \tag{2}$$

Here Ω is the unit-cell volume, $\hbar\omega_{nm} = E_n - E_m$ is the energy difference between occupied (E_m) and unoccupied (E_n) bands. The parameter δ represents the broadening of the spectral lines due to a finite lifetime of the excited states. In general δ is a function of ω which can be in principle calculated from the many-body theory. Such a calculation is beyond the scope of the present paper and thus we treat δ as a phenomenological parameter. Π^{α}_{nm} are the momentum matrix elements given by

$$\Pi^{\alpha}_{nm}(\boldsymbol{k}) = \int_{\Omega}\psi_{n\boldsymbol{k}}(\boldsymbol{r})\,p^{\alpha}\psi_{m\boldsymbol{k}}(\boldsymbol{r})\,\mathrm{d}\boldsymbol{r} \tag{3}$$

which represent a non-relativistic approximation to the dipolar transition matrix elements [2].

The band structure represented by a set of eigenvalues $E_n(\boldsymbol{k})$ and eigenvectors $\psi_n(\boldsymbol{k})$ on a k-point mesh in the Brillouin zone is required as an input for the evaluation of equation (2). After the evaluation of the matrix elements Π^{α}_{nm}, k-space integration divided into two steps is performed. In the first step we integrate over surfaces of constant $\omega_{nm}(\boldsymbol{k}) = \omega'$, which corresponds to calculation of the absorptive part of $\sigma_{\alpha\beta}(\omega)$ in the limit $\delta = 0$. The Blöchl tetrahedron method is used here. The second integration is over ω' and it corresponds to performing Kramers–Kronig transformation and lifetime broadening. It is well known that Kramers–Kronig transformation suffers from inaccuracy due to necessity of a high-energy cut-off for the absorptive part of the conductivity [13]. We found that an energy cut-off at

2.0 Ryd and an energy mesh of 1 mRyd yields satisfactory convergence for the spectrum up to 0.6 Ryd.

The FPLAPW method is used for the band-structure calculation. Within this method the unit cell is divided into non-overlapping atomic spheres and an interstitial space. The potential is expanded into spherical harmonics inside the atomic spheres and into plane waves in the interstitial space. Similar expansion is used for the basis functions. The spin–orbit coupling is included by the second-variational step [9] inside the atomic spheres using the spherical part of the potential, i.e. muffin-tin approximation to the spin–orbit coupling. This means that the Hamiltonian without the spin–orbit coupling is diagonalized first. Then an energy cut-off is made and only the states under this spin–orbit cut-off energy are used as a basis for diagonalization of the Hamiltonian including the spin–orbit coupling. This procedure is faster compared to the direct inclusion of the spin–orbit coupling into the Hamiltonian as used in [12]. The accuracy of these approaches is the same for high enough energy cut-off but the second-variational-step approach is still several times faster. For the discussion of the energy cut-off, see section 3.2.1.

2.1. Orbital polarization

The local spin-density approximation leads to a considerable underestimation of the orbital momentum for Fe and Co [6] and it is likely that the MOKE is also strongly influenced. The orbital momentum may be enhanced by inclusion of the orbital polarization term [7], which mimics the second Hund rule:

$$\begin{aligned} \hat{H}_{OP} &= H_{orb}\hat{l}_z \\ H_{orb} &= -I_{OP}L_z \end{aligned} \tag{4}$$

where $\hat{l}_z$ is the z-component of the angular momentum operator, the z-axis being parallel to the magnetization, and L_z is the projection of the orbital moment on the z-axis:

$$L_z = \sum_{i,\boldsymbol{k}} n_{i,\boldsymbol{k}} \langle \psi_{i,\boldsymbol{k}} | l_z | \psi_{i,\boldsymbol{k}} \rangle. \tag{5}$$

$\psi_{i,\boldsymbol{k}}$ is the eigenstate of an energy band i with a wave vector $\boldsymbol{k}$; $n_{i,\boldsymbol{k}}$ are the occupation numbers. Finally the parameter I_{OP} is equal to the Racah parameter B for the d electrons and E^3 for the f electrons (see e.g. [8]). Racah parameters are easily calculated once the wave functions inside the atomic spheres are known. Alternatively they may be obtained from the analysis of optical spectra. In the present calculation the values $B = 0.100$, 0.099 and 0.127 eV for Fe, Co and Ni, obtained by the latter method [8], are used.

In our computational scheme $\hat{H}_{OP}$ is treated using the second-variational method [9], i.e. in the same way as the spin–orbit coupling in the WIEN97 package. However, $\hat{H}_{OP}$ is proportional to the orbital momentum operator $\hat{l}_z$ and at the same time H_{orb} in front of this operator contains matrix elements of $\hat{l}_z$. An additional self-consistency loop must therefore be added into the computational scheme. In the first step L_z is calculated using the eigenfunctions of the Hamiltonian $\hat{H}_0$ which does not contain the orbital polarization term. $\hat{H}_{OP}$ is then determined using (4) and the eigenfunctions of $\hat{H}_0 + \hat{H}_{OP}$ are found. L_z is calculated in the new basis and the new $\hat{H}_{OP}$ is constructed. The procedure is repeated until the self-consistency is reached. We found that for the systems in question the procedure converges fast and no mixing of the intermediate results is necessary.

3. Results

3.1. Comparison with the ASW method and with experiment

In this section the calculated MOKE spectra are compared to the results obtained by the ASW method [2, 19] and to the experimental data. All calculations are performed for the magnetization parallel to the [001] direction. The simultaneous presence of the spin–orbit coupling and the magnetization then lowers the symmetry of Ni and Fe, while the symmetry group of hcp Co remains unchanged. The program may be equally well applied for an arbitrary direction of the magnetization. This leads, however, to further lowering of the symmetry resulting in a larger irreducible wedge of the Brillouin zone and correspondingly higher demands on the computer memory and time. To make detailed comparison possible the same inputs as in references [2, 19] are used for the lattice parameters of the systems in question and for the lifetime broadening. The lattice constants for fcc Ni and bcc Fe are 0.352 43 nm and 0.286 62 nm, respectively. For hcp Co $a = 0.260\,35$ nm and $c = 0.422\,81$ nm are used. The same lifetime broadening $\delta = 0.4$ eV is assumed for all three systems. Also the form of the LSDA exchange–correlation potential is analogous—we use the Perdew and Wang [10] reparametrization of the Ceperley–Alder data. In all cases the calculation is driven to self-consistency (the change of the total energy in subsequent iterations is smaller than 10^{-6} Ryd). The spin–orbit coupling is included in the self-consistent iteration procedure. Electron states are divided into core states (1s, 2s, 2p, 3s) and valence states (3d, 4s, 4p); the 3p orbitals are treated as local orbitals [9].

The results for bcc Fe, hcp Co and fcc Ni are displayed in figures 1, 2 and 3. The comparison of the MOKE spectra to other experimental and computational studies is discussed here. In all three cases we found good agreement with the calculations of Oppeneer *et al* [2, 19]. Compared to the experimental data an agreement as regards the shape and the magnitude can be found in all three cases. Inclusion of the intraband contribution to the diagonal elements of the conductivity tensor would improve this agreement in the low-energy region (below 2 eV). Some discrepancies still remain, especially overestimation of the crossover energy of the Kerr rotation in Ni around 4 eV. For a detailed discussion see [3]. For Ni and Fe we compared our results also to the calculations of Delin *et al* [4] and Mainkar *et al* [11]. Both these calculations used the full potential. Because these calculations used a different lifetime broadening and

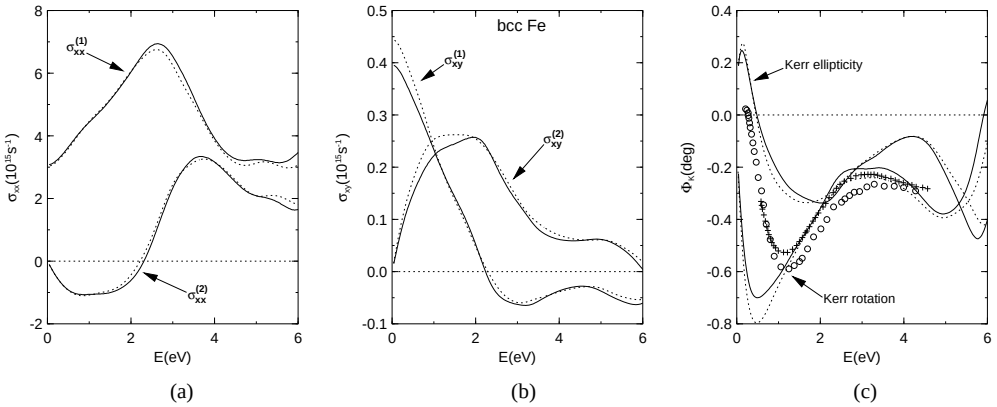

Figure 1. Theoretical conductivity tensor elements σ_{xx} (a), σ_{xy} (b) and theoretical and experimental MOKE spectra (c) for bcc Fe. The results are shown as follows: solid curve: this work; dotted curve: Oppeneer and Antonov [3]; +: van Engen [21]; ○: Krinchik and Artem'ev [14].

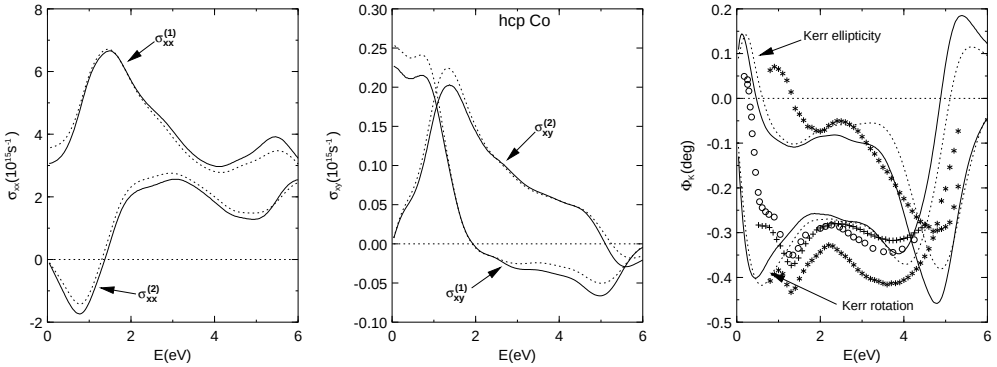

Figure 2. Theoretical conductivity tensor elements σ_{xx} (a), σ_{xy} (b) and theoretical and experimental MOKE spectra (c) for hcp Co. The results are shown as follows: solid curve: this work; dotted curve: Oppeneer and Antonov [3]; +: van Engen [21]; ○: Krinchik and Artem'ev [14]; ∗: Weller *et al* [17].

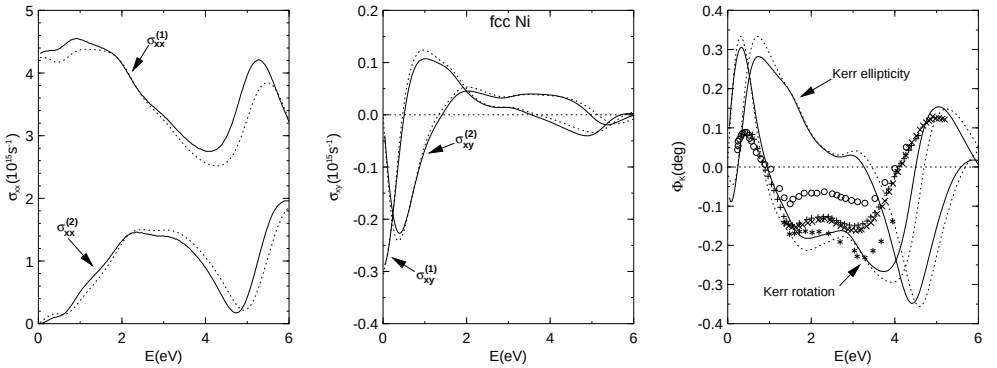

Figure 3. Theoretical conductivity tensor elements σ_{xx} (a), σ_{xy} (b) and theoretical and experimental MOKE spectra (c) for fcc Ni. The results are shown as follows: solid curve: this work; dotted curve: Oppeneer and Antonov [3]; +: van Engen [21]; ○: Krinchik and Artem'ev [14]; ∗: data of Di and Uchiyama [16] with compensation for the quartz substrate given by Di [15]; ×: Višňovský *et al* [20].

included the intraband conductivity, only major differences which are not affected by this fact are mentioned. Unlike Delin *et al* we found crossover to positive values of the Kerr rotation at about 4.5 eV for Ni and 6 eV for Fe. The difference is even more striking for the Kerr ellipticity where we found crossovers to positive values at about 5 eV for Ni and 7 eV for Fe. Comparing to the results of Mainkar *et al* a good agreement up to 6 eV exists for Fe, while in the case of Ni our results are closer to those of Oppeneer *et al* above 3 eV.

3.2. The influence of the input parameters

In this section the influence of the choice of the basis set for the wave functions, the expansion of the potential and the number of k-points in the irreducible wedge of the Brillouin zone on the theoretical MOKE spectra is analysed. In order to compare conveniently the dependence of the Kerr rotation and ellipticity for two values P_1, P_2 of the input parameter P, we introduce

the quantity χ which characterizes the overall change of the spectrum and Δ, indicating the maximum difference:

$$\chi = \int_0^{E_m} |A_{P_1}(E) - A_{P_2}(E)|/|A_{P_2}(E)| \, \mathrm{d}E \qquad E = \hbar\omega \qquad A = \Theta_K, \Phi_K$$
$$\Delta = \max(|A_{P_1}(E) - A_{P_2}(E)|/|A_{P_2}(E)|) \tag{6}$$

where E_m is the maximum value of the energy in the Kerr spectrum. In what follows we use $E_m = 6$ eV. The testing was performed mostly on hcp Co and its results were taken into account for the other systems. The procedure was the following. The band-structure calculation was driven to self-consistency with the spin–orbit cut-off energy about 1 Ryd above the Fermi energy, then this energy was increased and the band structure used for the determination of the MOKE spectrum was calculated again with higher-lying states included.

3.2.1. The basis set for the wave functions and potential. Within the LAPW method the number of basis functions is limited by the magnitude of the largest $\boldsymbol{k}$-vector in the plane-wave expansion. In the WIEN code the $\boldsymbol{k}$-vector cut-off is characterized by the product $p = R_{mt}K_{max}$ where R_{mt} is the radius of the smallest atomic sphere and K_{max} is the maximum value of the wave vector. We note that when the number of plane waves is increased, so should the number of spherical harmonics inside the atomic spheres be increased; these are characterized by an angular momentum cut-off value L_{max}. The default WIEN values are $p = 8$ and $L_{max} = 10$. The comparison with the calculations for $p = 10$, $L_{max} = 12$ gives maximum deviations of $\Delta(\Theta_K) = 10.3\%$, $\chi(\Theta_K) = 4.1\%$, which decrease to 4.1% and 2.6% for $p = 9$, $L_{max} = 11$. In what follows we take $p = 10$, $L_{max} = 12$ as our default values.

The second-variational method adds another parameter which is the spin–orbit cut-off energy (see section 2). We found that there is an influence of the states lying above the range used in the calculation of the MOKE spectrum, i.e. 2 Ryd above the Fermi level, due to hybridization with the states included in this calculation. Taking the value $E_{max} = 9$ Ryd as a reference, we found that for $E_{max} = 5$ Ryd the deviations are already below 0.5%, thus indicating reliability of the second-variational method.

In the WIEN code the expansion of the potential is characterized by a parameter G_{max} determining the magnitude of the largest reciprocal-space vector used. The WIEN default value $G_{max} = 10$ should be increased for the calculation using the GGA. We therefore increased G_{max} to 14, but there is only little difference comparing to the $G_{max} = 12$ calculation.

Because the spin–orbit coupling is considered inside the atomic spheres only, the dependence on the sphere radii R_{mt} should be checked. Note that most of the other results obtained by the WIEN code are not sensitive to the choice of R_{mt}, provided that the parameters $p = R_{mt}K_{max}$ and G_{max} are sufficiently large. We checked the sensitivity of the theoretical MOKE spectrum and the orbital momentum to the choice of R_{mt} for fcc Ni. The deviation of the MOKE spectrum characterized by parameters χ and δ caused by reduction of the maximum allowed R_{mt} (almost touching spheres) by 12% was less than 2%. At the same time the orbital momentum decreased by almost 5%. These results justify using the muffin-tin approximation to the spin–orbit coupling in the calculation of the MOKE.

For hcp Co and fcc Ni we also performed calculations in which the 3p states were kept in the core. This led to a downward shift of Θ_K of $\approx$0.05–0.1° for Co and 0.01–0.5° for Ni, while the shape of the spectra remained unchanged.

3.2.2. The number of k-points. The same number n_k of k-points in the irreducible wedge of the Brillouin zone was used in the self-consistency cycles and in subsequent calculation of the MOKE spectrum. Testing of the dependence of the results on n_k was performed for all three

systems. We found that the character of the spectra (number and positions of maxima and minima) is already relatively stable for moderate n_k. In order to achieve deviations ≈1–4%, large n_k may be needed, however. For hcp Co this fact is demonstrated in table 1. In the case of bcc Fe, 1183 k-points already yields good stability. In case of Ni, the MOKE spectrum is reasonably stable for 3078 k-points although the diagonal conductivity, especially, still varies in the region below 1 eV. This could explain the deviation from the previous calculation [2] in this energy region, but the differences of the MOKE spectra at higher energies are independent of this fact.

Table 1. The dependence of χ and δ on the number of k-points n_k for hcp Co; the calculation with 1540 k-points was taken as a reference.

	Kerr rotation		Kerr ellipticity	
n_k	χ	δ	χ	δ
240	0.07	0.10	0.06	0.04
427	0.03	0.15	0.06	0.07
819	0.01	0.03	0.02	0.01

3.3. The influence of the exchange–correlation potential and orbital polarization

The MOKE spectra obtained with the use of the GGA exchange–correlation potential and with the orbital polarization term in the Hamiltonian as described in section 2.1 are compared in figure 4. In table 2 we also present the orbital moments calculated with and without the orbital polarization.

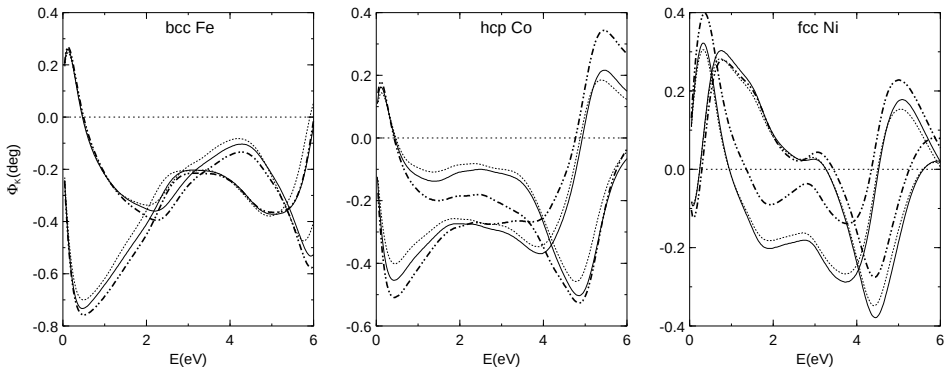

Figure 4. MOKE spectra calculated with the LSDA (dotted curves) and GGA (solid curves) exchange–correlation potentials. Dash–dotted curves correspond to the calculation including the orbital polarization.

It can be seen that use of the GGA exchange–correlation potential leads to increasing of the amplitude of the Kerr rotation and ellipticity in all three cases. However, this change is small and does not remove the main discrepancies between the calculation and the experiment. Thus it can be stated that the use of the GGA does not improve the description of reality as compared to LSDA for the systems studied.

It is well known that the inclusion of the orbital polarization leads to increasing of the orbital moment to values closer to the experimental ones [7]. This is also shown in table 2.

Table 2. The orbital moments calculated with and without the orbital polarization.

	Orbital moment (μ_B)	
	Without OP	With OP
Fe	0.045	0.063
Co	0.107	0.160
Ni	0.051	0.066

On the other hand the MOKE spectra obtained with the orbital polarization are further from the experimental ones, which is readily seen for Ni and Co.

4. Conclusions

We have presented a calculation of the polar magneto-optical Kerr effect in bcc Fe, hcp Co and fcc Ni using the full-potential linearized augmented-plane-waves method. We found a close agreement with the results obtained by the ASW method [2, 19]. As both of the methods use the local spin-density approximation to the density functional theory, we conclude that the remaining deviations from the experiment come from the LSDA itself rather than from mathematical approximations made within the different methods of band-structure calculation. We checked the sensitivity of the calculated MOKE spectra to the parameters of the calculation and found the values for which reasonably stable results are obtained. We also showed that the muffin-tin approximation and the second-variational treatment of the spin–orbit coupling are justified for the present calculations.

Acknowledgments

We are indebted to P M Oppeneer for helpful discussions and providing us with his computational results. We also appreciate correspondence with C Ambrosch-Draxl and discussion with P Blaha. This work was supported by the grant A1010715/1997 of the Grant Agency of AV ČR and partially also by grant No LB98202 within the project INFRA2 of the Ministry of Education, Youth and Sports of the Czech Republic.

References

[1] Wang C S and Callaway J 1974 *Phys. Rev.* B **9** 4897
[2] Oppeneer P M, Maurer T, Sticht J and Kübler J 1992 *Phys. Rev.* B **45** 10 924
[3] Oppeneer P M and Antonov V N 1996 *Spin–Orbit-Influenced Spectroscopies of Magnetic Solids* ed H Ebert and G Schütz (Berlin: Springer) p 29
[4] Delin A, Eriksson O, Johansson B, Auluck S and Wills J M 1999 *Phys. Rev.* B at press
[5] Blaha P, Schwarz K and Luitz J 1997 *WIEN 97* Vienna University of Technology
This is an improved and updated Unix version of the original copyrighted WIEN code, which was published by Blaha P, Schwarz K, Sorantin P and Trickey S B 1990 *Comput. Phys. Commun.* **59** 399
[6] Söderlind P, Eriksson O, Johansson B, Albers R C and Boring A M 1992 *Phys. Rev.* B **45** 12 911
[7] Eriksson O, Johansson B and Brooks M S S 1989 *J. Phys.: Condens. Matter* **1** 4005
[8] Griffith J S 1961 *The Theory of Transition-Metal Ions* (Cambridge: Cambridge University Press)
[9] Singh D J 1994 *Plane Waves, Pseudopotentials and the LAPW Method* (Dordrecht: Kluwer Academic)
[10] Perdew J P and Wang Y 1992 *Phys. Rev.* B **45** 13 244
[11] Mainkar N, Browne D A and Callaway J 1996 *Phys. Rev.* B **53** 3692
[12] Dewitz J P, Chen J and Hübner W 1998 *Phys. Rev.* B **58** 5093
[13] Gasche T, Brooks M S S and Johansson B 1996 *Phys. Rev.* B **53** 296

[14] Krinchik G S and Artem'ev V A 1968 *Sov. Phys.–JETP* **26** 1080
[15] Di G Q 1995 private communication to P M Oppeneer
[16] Di G Q and Uchiyama S 1994 *J. Appl. Phys.* **75** 4270
[17] Weller H Y, Harp G R, Farrow R F C, Cebollada A and Sticht J 1994 *Phys. Rev. Lett.* **72** 2097
[18] Guo G Y and Ebert H 1995 *Phys. Rev.* B **51** 12 633
[19] Oppeneer P M, Sticht J, Maurer T and Kübler J 1992 *Z. Phys.* B **88** 309
[20] Višňovský Š, Pařízek V, Nývlt M, Kielar P, Prosser V and Krishnan R 1993 *J. Magn. Magn. Mater.* **127** 135
[21] van Engen P G 1983 *PhD Thesis* Technical University of Delft